



Evaluation of the mechanical properties of T91 steel exposed to Pb and Pb–Bi at high temperature in controlled environment

B. Schmidt, S. Guerin, J.-L. Pastol, P. Plaindoux, J.-P. Dallas,
C. Leroux, D. Gorse *

CNRS–CECM, 15 rue Georges Urbain, Vitry/Seine 94407, France

Abstract

It is known that liquid metal embrittlement (LME) is strongly dependent on a so-called ‘intimate contact’ between the solid and liquid metal (LM) phases. This point is emphasised in this paper aimed at determining suitable contact conditions to favour LME of T91 steel after short exposure to stagnant molten Pb or Pb–55%Bi. The temperature range ($T \sim 540^\circ\text{C}$) is high with respect to the expected operating conditions of spallation targets. We determine three temperature cycles, in pure lead or lead–bismuth under flowing He–4% H_2 for LME testing. Good contact is obtained between T91 and Pb–Bi, but poor contact between T91 and Pb. Accordingly, the T91 steel tensile properties are not degraded by Pb, but modified after exposure to Pb–Bi. In such case, rupture of the test bar occurs in regions where Pb–Bi is ‘adherent’ onto the steel. The rupture facies is not fully ductile as for T91 in Pb. © 2001 Elsevier Science B.V. All rights reserved.

1. Introduction

In order to validate the concept of liquid metal (LM) target for accelerator driven systems (ADS), the choice of both the structural materials and of the LM target must be optimised [1]. To be more specific, as structural materials for the target window, 9%Cr martensitic steels, like EM10 (9%Cr1%Mo) or T91 (9%Cr1%MoVNb), satisfy a priori the required metallurgical criteria under irradiation. On the other hand, the LM must be a satisfying spallation neutron source and maintain the durability of the target structural materials at long term (months to year). In other words, the resistance to corrosion and liquid metal embrittlement (LME) of structural materials for the LM target of the spallation neutron source in ADS must be carefully investigated, without and under proton irradiation.

Satisfying thermodynamics and neutronics criteria, molten Pb and Pb–Bi are potential candidates for the

LM target. Their compatibility with 9%Cr martensitic steels remains to be determined [2].

In this paper, our purpose is to determine whether or not it is possible to embrittle one of the pre-selected martensitic steels, namely T91 steel, in molten Pb and/or Pb–Bi by simply varying the temperature and the contact conditions between the solid and liquid phases.

LME is defined as the degradation of the mechanical properties of otherwise ductile metal induced by some interaction with a LM and under mechanical sollicitation [3,4]. We recall that Fe–Pb and Fe–Bi are not known to be embrittling couples [5]. The same observation can be made with steel in lead alloys. However, the signature of an embrittling effect of lead (reduction of area, plastic strain at rupture, UTS) is well mentioned in some cases. For example, it is the case of leaded steels [6,7], of 8–9%Cr martensitic steels after some specific heat treatments [8]. On the other hand, it was shown recently that notched specimens exhibit brittle rupture under particular metallurgical and mechanical testing conditions [9].

We show that, under the present experimental conditions, for all tested temperature cycles, intimate contact cannot be obtained between T91 steel and lead and that T91 steel is not embrittled by lead. Turning to Pb–

* Corresponding author. Tel.: +33-1 56 70 30 61; fax: +33-1 46 75 04 33.

E-mail address: dominique.gorse@glvt-cnrs.fr (D. Gorse).

Bi, it appears that the interactions with the steel surface are drastically modified, for at least two temperature cycles, always after short exposure time to Pb–Bi. A beginning of change in the tensile properties is revealed. Those findings suggest intricate T91 steel interactions with molten lead–bismuth of eutectic composition susceptible to lead to significant changes in the metallurgical properties of the system. One may wonder whether there is a bismuth concentration threshold to observe variations in the compatibility of 9%Cr martensitic steels with the molten metal bath.

2. Experimental

Tensile specimens (4 mm in diameter and 15 mm of gauge length) and rectangular samples ($20 \times 10 \times 4 \text{ mm}^3$) are prepared from steel T91 provided by Creusot Loire Industrie (CLI) whose composition is given in Table 1.

The as-received T91 steel specimens are normalised by 1/2 h austenitisation at 1050°C , air-quenched, and then tempered for 1 h at 750°C . As a result, a martensitic microstructure is obtained while the grain size of the prior austenite phase is about $20 \mu\text{m}$ [10]. Coarse polishing of the rectangular samples is done with Struer's PIANO 120 diamond disk, followed by fine polishing with 10, 6, 3, and $1 \mu\text{m}$ sized diamond particles. Rectification of the tensile specimens is done down to a $0.4 \mu\text{m}$ rugosity.

The lead of 99.995% purity (main impurities: 0.002% Ag, 0.001% Cu, 0.0015% Fe and 0.0002% As) was mechanically cleaned and chemically ($1/3 \text{ H}_2\text{O}_2$, $1/3$ acetic acid, $1/3$ ethanol) degreased for 5 min. Supplied by Metaleurop, the Pb–Bi alloy of eutectic composition ($x_{\text{Pb}} = 0.45 \text{ wt}\%$) and 99.99% purity (main impurities: 0.0006% Ag, $<0.0003\%$ Te, $<0.0001\%$ Ni, $<0.0002\%$ Cu, Cd, Sb, Sn, As) is previously purified by HF melting. This last treatment is justified by a high gas content found in the Pb–Bi ingot.

Two testing procedures are investigated: (a) either the steel specimens and the Pb or Pb–Bi ingots are heated together in an horizontal boron nitride-coated alumina crucible or (b) the test bar (kept at room T) is immersed by vertical translation in the molten bath heated at the desired temperature. Three temperature cycles of short duration are applied as schematised in Fig. 1. A 2 h decrease back to room temperature is programmed.

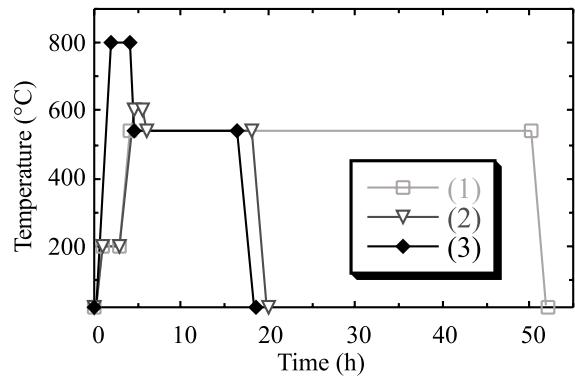


Fig. 1. Thermal cycle applied to steel T91 in molten Pb (1, 2), Pb–Bi (2,3): (1) 2 h at 200°C , then 48 h annealing at 540°C followed by slowly cooling in the oven; (2) 2 h at 200°C , then 1 h at 600°C followed by 12 h annealing at 540°C and cooling in the oven; (3) same as (2) except that there is only one pre-heating step of 1 h at 800°C .

However, thermal inertia of the oven resulted in a real cooling time of 4–5 h.

Thermal cycle (3) begins by 1 h at 800°C . In such a case, the steel microstructure is kept, but carbides may begin to coalesce, leading to a possible slight degradation of the mechanical properties. This heat treatment should not be visible on tensile tests, but affect only slightly the toughness level.

In all cases, the heat treatment was carried out under flowing He-4\%H_2 , with a residual water vapour content less than 15 vppm. The gas circulation begins once the vacuum of the sample holder is less than 10^{-5} Torr. No other oxygen control system, such as an electrochemical pump, is used in the molten bath [11].

The specimens are examined post-mortem using a Schottky source field effect emission SEM (LEO 1530) with a zirconia-coated tungsten tip. For a beam energy as low as 3 keV, typical resolution is about 3 nm.

Rectangular samples of size $20 \times 10 \times 4 \text{ mm}^3$ are analysed by grazing incidence X-ray diffraction (XRD) using a standard Philips diffractometer (PW1830 generator: 40 kW, 30 mA, wavelength: $\lambda(\text{Co, K}_\alpha) = 1.7902 \text{ \AA}$). Operating conditions are as follows: 1° divergence slit, no monochromator, step angle 0.035° , sample time 85 s, angular range, $20\text{--}80^\circ$. Decreasing graze angles ($0.15^\circ \leq \theta \leq 0.35^\circ$) are employed to determine the composition of the uppermost surface layers (few nm).

Table 1
Composition of T91 steel (wt%, balance Fe)

C	Mn	P	S	Si	Cr	Mo	Ni
0.105	0.38	0.009	0.003	0.43	8.26	0.95	0.13
V	Nb	N ₂	Al	Cu	As	Sn	Ti
0.2	0.08	0.055	0.024	0.08	0.02	0.008	0.014

Mechanical tests are performed at room temperature on an electromechanical machine (MTS 20/M type). Deformation levels are determined by using a MTS micro-extensometer directly placed on the gauge length of the specimen.

3. Results and discussion

Very recently, in the frame of the European research projects related to ADS, was studied the long-term corrosion behaviour (in the range 800–3000 h) of martensitic and austenitic steels in lead or lead alloys under stagnant [12,13] conditions in the temperature range expected in ADS.

In this study, we are only concerned by the mechanical behaviour of T91 after short exposure times (few hours) to stagnant molten lead or lead–bismuth maintained at high temperature: 540°C on the average preceded or not by 1 h annealing at 600°C or 800°C. This prior annealing of one hour is simply carried out to change the contact conditions at the steel–LM interface. It is not our purpose to discuss here the slight modification of the distribution of carbides in the bulk T91 steel test bar, made possible by 1 h at 800°C and of no consequence on the tensile behaviour.

In all testing conditions, the use of flowing He–4% H_2 is not sufficient to prevent PbO formation, as seen in the XRD spectra of Fig. 2. The temperature of 540°C is that of the transformation of PbO-L (Litharge) to PbO-M (Massicot), as shown in Fig. 2(b). The oxygen potential is fixed by the Pb/PbO equilibrium. According to the Ellingham diagrams, the partial pressure of oxygen should be in the range of $\sim 10^{-17}$ atm. Moreover, the oxides usually found on Cr-containing steels, like Fe_2O_3 , Fe_3O_4 , Cr_2O_3 , Cr_3O_4 , $(Fe_{0.6}Cr_{0.4})_2O_3$, $FeCr_2O_4$, are absent from all XRD spectra, even when varying the graze angle, suggesting the presence of just a very thin oxide layer, too thin to

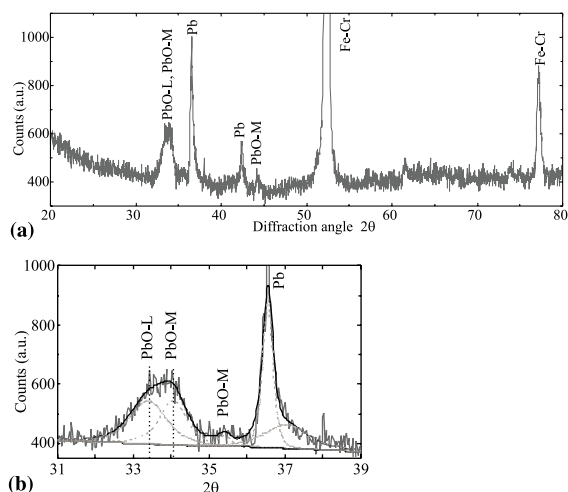


Fig. 2. Grazing angle ($\theta = 0.2^\circ$) XRD spectrum of T91 steel in molten Pb following procedure (1): total spectrum in (a), zoom in 'PbO region' in (b).

be observable. The nature of the oxide layers was qualitatively obtained by EDS analysis.

3.1. T91 steel–Pb system

As shown in Fig. 3, there is no 'intimate contact' between lead and T91 steel under the present operating conditions when applying the temperature cycle (1). No effect of the testing procedure is observed, without (a) or with (b) prior melting of lead. In this early stage of oxide growth, acicular crystallites of iron oxide are clearly visible in Fig. 3. Moreover, solidification of molten lead invariably gives rise to Pb droplets whose size ranges from a few to hundreds of nanometers. Their size and size distribution are apparently functions of the temperature cycle chosen. The minimum size of the droplets decreases, and the size distribution broadens on

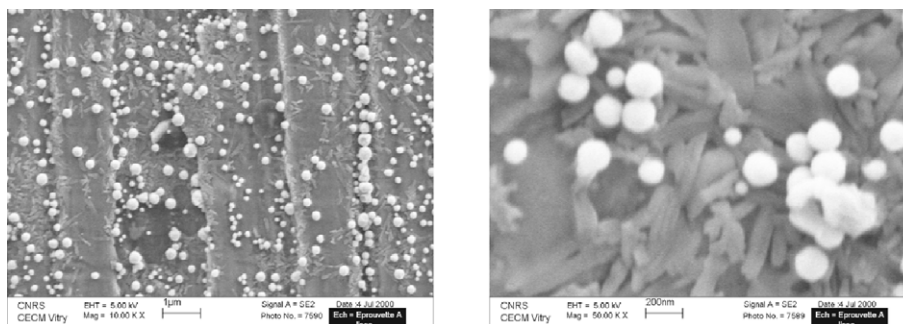


Fig. 3. SEM micrographs of T91 steel after 48 h immersion in molten Pb at 540°C under flowing He–4% H_2 . Lead ingots and steel are heated at the same time in a boron nitride-coated horizontal crucible. Left: typical view of steel surface; right: zoom showing lead droplets on the slightly oxidised surface, in the form of iron oxide needles.

increasing the maximum temperature of the molten lead bath. Accordingly, applying cycle (1) or (2), only the apparent distribution of the lead droplets is varied but the overall post-mortem aspect of the steel surface is unchanged.

Consequently, the tensile behaviour of lead-treated T91 steel is very similar to that of a reference specimen in air (Fig. 7). Ductile failure is observed with an elongation to failure in the range of 40%.

Indeed, the wetting transition temperature should be expected to occur at a much higher temperature for a 9%Cr-containing steel, possibly only under UHV. One should also account for the possible Si segregation in uppermost surface layers susceptible to modify the wetting transition temperature (see the Si content of the steel in Table 1).

However, applying temperature cycle (1), lead sticking onto the T91 steel surface was observed, with adherence to the steel surface proved by ductile rupture

during extraction of the steel sample from the solidified lead ingot [14].

At this point, the question remains as to the possibility of obtaining a good contact with the T91 steel–Pb couple. And even in that case, would it be a sufficient condition to permit the occurrence of LME?

3.2. T91 steel–Pb–Bi system

Thermodynamically, referring to the available equilibrium phases diagrams (Fe–Pb or Fe–Bi, Cr–Pb or Cr–Bi) and other related data (inter-diffusion, wetting properties), significant changes in the contact conditions were a priori unexpected by changing the nature of the molten bath, from Pb to Pb–Bi [15]. However, in otherwise identical experimental conditions, especially referring to the oxygen level, the thermodynamics of the T91–Pb–Bi system is unknown.

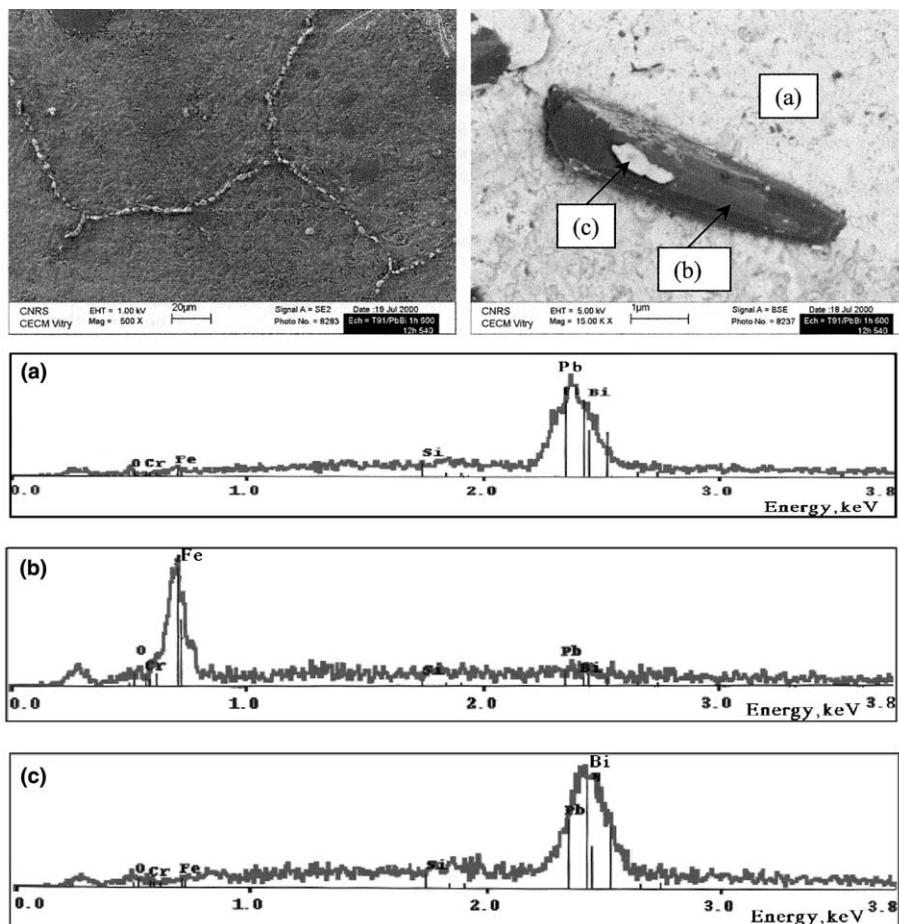


Fig. 4. SEM micrographs of T91 steel in molten Pb–Bi following procedure (2). Lead ingots and steel are heated at the same time in a boron nitride-coated horizontal crucible. Left: typical top view of steel surface; right: zoom showing a crystallite of iron decorating some GB revealed by immersion in Pb–Bi. The EDS analysis of the right micrograph is shown below.

Note that there are also intriguing features appearing when one compares wetting or susceptibility to LME of various metals with either Pb or Bi. Solid Cu and Ni are not embrittled by lead, but significantly by bismuth. To our knowledge, there is a lack of information concerning the interactions between Fe and Bi. Wettability of Fe by molten Bi was scarcely observed above 600°C in the 1930s [15].

Fig. 4 shows a top view of the T91 steel surface after exposure to molten Pb–Bi, following testing procedure (a) and temperature cycle (2). The first noticeable point

is that Pb–Bi is now apparently adherent to the steel surface (see EDS spectrum noted (a) in Fig. 4). This makes already a significant difference with the T91–Pb system. Apparently, the grain boundaries (GB) are now visible, since they are decorated by iron crystallites (see EDS spectrum noted (b) in Fig. 4). Moreover, it seems that bismuth plays a particular role in the formation of these crystallites since apparently lead-free bismuth is observed in close contact with the Fe crystallites (see EDS spectrum noted (c) in Fig. 4), when observable. This result suggests penetration of bismuth into some

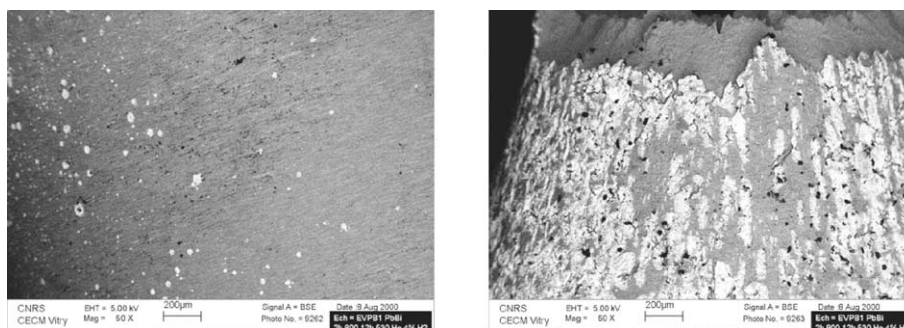


Fig. 5. SEM micrographs showing lateral views of T91 steel tensile specimen immersed in molten Pb–Bi following testing procedure (b) and temperature cycle (3). Note that the rupture occurs in regions of ‘good contact’ with molten Pb–Bi (right: bright area), and apparently not in regions of ‘poor contact’ with Pb–Bi (left: white spots spread at random on the tensile specimen).

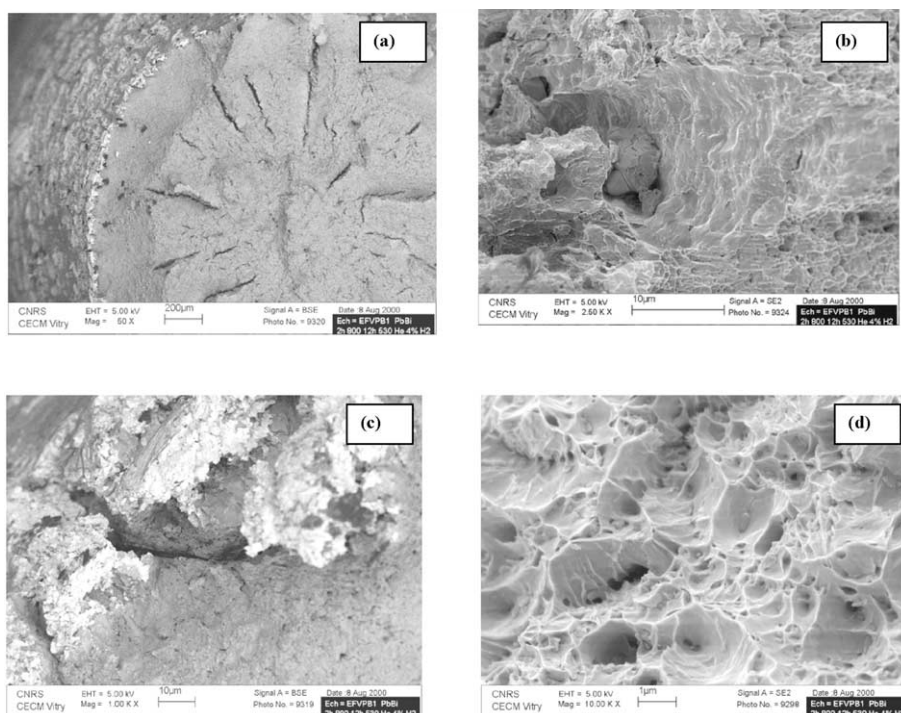


Fig. 6. SEM micrographs showing a typical rupture facies (a) of T91 in molten Pb–Bi following testing procedure (b) and cycle (3): showing a ductility loss at the periphery (b,c), but always ductile at the centre (d).

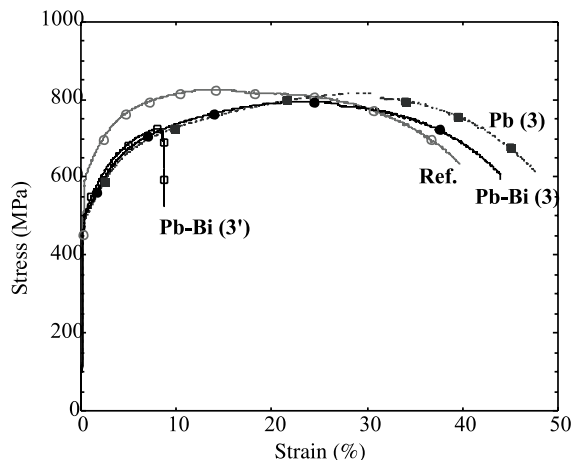


Fig. 7. Stress–strain plots obtained at $\dot{\epsilon} = 2 \times 10^{-4} \text{ s}^{-1}$ on steel T91: (i) normalised and tempered (Ref.), (ii) heat-treated in molten Pb following testing procedure (a) and temperature cycle (3), referred to as Pb (3), (iii) same as (ii) in molten Pb–Bi referred to as Pb–Bi (3), (iv) heat-treated in molten Pb–Bi following testing procedure (b) and temperature cycle (3), referred to as Pb–Bi (3').

GB of the steel, in spite of the unavoidable presence of an interfacial oxide.

Testing procedure (b) together with application of temperature cycle (3) confirmed those findings. The main results of the tensile tests are summarised in Figs. 5–7.

During tensile tests conducted at $\dot{\epsilon} = 2 \times 10^{-4} \text{ s}^{-1}$ on specimens of T91 steel after immersion in Pb–Bi following procedure (b) and heat-treatment of 1 h at 800°C followed by 12 h at 540°C, the rupture occurs in regions of ‘good contact’ with Pb–Bi, and not in regions of ‘poor contact’ with Pb–Bi (Fig. 5). Apart from the fact that this result reveals that the T91–Pb–Bi contact is not homogeneous over the whole surface of the test bar, this observation suggests a correlation between the presence of Pb–Bi and the onset of cracking. The inhomogeneous T91–Pb–Bi contact could be at least partially explained by an also inhomogeneous thin oxide layer of varying composition at the steel surface, once remarked that 1 h at 800°C is sufficient to induce Si segregation in the surface layers and that the composition of the surface oxide may vary from the Si-rich area to the Fe-rich area, whose interaction with molten Pb–Bi is unknown. As concerns the post-mortem failure of T91 steel in Pb–Bi-rich area observed in Fig. 5, this observation suggests to draw a parallel with the solid metal-induced embrittlement (SMIE) of 4140 steel by indium [16]. In these experiments, application of an indium band (4 mm wide and 0.25 mm thick) produces cracking in the indium-covered portion of the sample gauge length. However, indium is an embrittler of steel [5], which is not expected

to be the case either of lead (as observed in this work) or of bismuth. Further work should be necessary to prove that bismuth can facilitate cracking and to determine its role and the required testing conditions.

A typical rupture facies is shown in Fig. 6(a). A loss of ductility is solely observable as a thin ring at the periphery of the fracture surface (Fig. 6(b)), often taking the form of large decohesions in regions of ‘adherent’ Pb–Bi (Fig. 6(c)). A large central region is ductile (Fig. 6(d)). This makes the difference with the rupture facies, always fully ductile observed with the T91–Pb system in the present testing conditions.

The corresponding stress–strain plots are reproduced in Fig. 7. The tensile behaviours of steel T91 in air after the same heat treatment (temperature cycle (3): 1 h at 800°C followed by 12 h at 540°C) using either the horizontal (specimens respectively referred to as Ref., Pb(3), Pb–Bi(3)) or vertical (referred to as Pb–Bi(3')) immersion procedure are compared. Note that the striction of Pb–Bi(3') occurred externally to the knives of the extensometer. For the optimal T91–Pb–Bi contact conditions obtained using testing procedure (b) and immersion in a Pb–Bi bath kept for 1 h at 800°C before decreasing back to 540°C (see Fig. 5), both the maximal stress and the corresponding strain decrease in comparison with the other above-mentioned testing conditions. The maximum stress reaches 750 and 800 MPa for Pb–Bi(3') and Pb–Bi(3), respectively. Likewise, the corresponding strain is reduced from 25% for Pb–Bi(3) to 8% for Pb–Bi(3'). Two points are worth mentioning. As expected, vertical immersion should improve the contact by minimising the role of the oxide that should be significant during melting of Pb or Pb–Bi ingots in the horizontal crucible. Rather unexpectedly, immersion in molten Pb–Bi at high T (800°C) modifies the tensile properties.

4. Conclusions

The influence of the contact conditions of both steel T91–Pb and T91–Pb–Bi systems on their tensile properties was studied at fixed oxygen potential. Only few hours of immersion of steel T91 in a stagnant molten bath are considered. The temperature of the molten bath is allowed to attain 800°C, that should be much higher than the in-service temperature conditions of the liquid metal target of ADS. The tensile properties are studied post-mortem. Consequently this work is concerned with embrittling conditions for SME rather than for LME.

Under conditions where the oxygen level is fixed by the Pb/PbO equilibrium, we have shown that:

- for the steel T91–Pb system, whatever the temperature cycle chosen, no contact is found due to the presence of an acicular iron oxide growing during the first

few hours of exposure to lead. Accordingly, no change in the tensile properties is observed, with respect to specimens only subjected to a similar heat-treatment.

- For the steel T91–Pb–Bi system, the contact is improved, and already good contact conditions are found with the temperature cycle (2) during which the temperature is raised for 1 h to 600°C. A change in the tensile properties is observed when the test bar is immersed by vertical translation in a molten Pb–Bi bath heated at 800°C for 1 h before decreasing to 540°C for 12 h. The rupture is seen in regions where Pb–Bi is adherent to the steel surface. The rupture facies resemble those obtained by SME for 4140 steel covered with indium.

Further work is necessary to determine more accurately the possible embrittling conditions of the T91–Pb–Bi system, considering the fact that bismuth, just as lead, is not known to be an embrittler of steel.

Acknowledgements

Financial support of the French GDR GEDEON is gratefully acknowledged. We are much indebted to Mr P. Bocquet from Creusot Loire Industrie for kindly providing the steel for all compatibility studies performed in the frame of the GDR GEDEON, and for always helpful discussions during the past four years.

References

- [1] C. Rubbia, J.A. Rubio, S. Buono, F. Carminati, N. Fiétier, J. Galvez, C. Gelès, Y. Kadi, R. Klapisch, P. Mandrillon, J.P. Revol, Ch. Roche, CERN/AT/95-44 (ET), 29 September 1995.
- [2] GEDEON Workshop on Materials for Hybrid Systems, 24–25 September 1997 (unpublished).
- [3] B. Joseph, M. Picat, F. Barbier, *Eur. Phys. J. AP* 5 (1999) 19.
- [4] E.E. Glickman, in: *Multiscale Phenomena in Plasticity*, NATO ASI Series E, vol. 367, 2000, p. 383.
- [5] A. Shunk, W.R. Warke, *Scr. Metall.* 8 (1974) 519.
- [6] W.R. Warke, K.L. Johnson, N.N. Breyer, in: J.E. Draley, J.R. Weeks (Eds.), *Corrosion by Liquid Metals*, Plenum, New York, 1970, p. 417.
- [7] S. Mostovoy, N.N. Breyer, *Trans. ASM* 61 (1968) 219.
- [8] T. Sample, H. Kolbe, *J. Nucl. Mater.* 283–287 (2000) 1336.
- [9] A. Legris, G. Nicaise, J.-B. Vogt, J. Foct, D. Gorse, D. Vançon, *Scr. Mater.* 43 (2000) 997.
- [10] P. Bocquet, Ph. Bourges, A. Cheviet, *Nucl. Eng. Des.* 144 (1993) 149.
- [11] V. Ghetta, F. Gamaoun, J. Fouletier, M. Hénault, A. Lemoulec, these Proceedings, p. 295.
- [12] G. Müller, G. Schumacher, F. Zimmermann, *J. Nucl. Mater.* 278 (2000) 85.
- [13] G. Benamati, P. Buttol, V. Imbeni, C. Martini, G. Palombarini, *J. Nucl. Mater.* 279 (2000) 308.
- [14] B. Schmidt, P. Plandoux, J.L. Pastol, D. Gorse, in: *Proceedings of the International Conference on Ageing and Life Time Extension of Materials*, Oxford, UK, 1999.
- [15] T.B. Massalski, et al., *Binary Alloy Phase Diagrams*, American Society for Metals, Cleveland, OH, 1990.
- [16] P. Gordon, H.H. An, *Metall. Trans.* 13A (1982) 457.